Influence of hydrogen adsorption on the optical properties of the GaAs(100)-$c(4 \times 4)$ surface

M. Arens
Institut für Festkörperphysik, Technische Universität Berlin, Hardenbergstraße 36, D-10623 Berlin, Federal Republic of Germany

M. Kuball and N. Esser
Max-Planck-Institut für Festkörperforschung, Heisenbergstraße 1, D-70569 Stuttgart, Federal Republic of Germany

W. Richter
Institut für Festkörperphysik, Technische Universität Berlin, Hardenbergstraße 36, D-10623 Berlin, Federal Republic of Germany

M. Cardona
Max-Planck-Institut für Festkörperforschung, Heisenbergstraße 1, D-70569 Stuttgart, Federal Republic of Germany

B. O. Fimland
Department of Physical Electronics, Norwegian Institute of Technology, N-7034 Trondheim, Norway
(Received 16 September 1994)

We have investigated the influence of hydrogen adsorption on the optical anisotropy and the surface reconstruction of the GaAs(100)-$c(4\times4)$ surface using reflectance difference spectroscopy (RDS) and low-energy electron diffraction (LEED), respectively. At low exposures the optical anisotropy of the $c(4 \times 4)$ surface is removed almost completely by hydrogen adsorption due to removal of the As dimers in the outermost As layer, while the LEED pattern changes from $c(4 \times 4)$ to (1×1). At intermediate hydrogen exposures, the surface again becomes optically anisotropic showing the signature of Ga dimers in the RDS spectra, while LEED indicates a mixture of (1×2) and $(\sqrt{2}\times\sqrt{2})$ reconstructions. Finally, at even higher dosages the Ga dimers are broken by hydrogenation. The LEED pattern shows a (1×1) symmetry and the RDS features are correlated with the critical points of the bulk electronic band structure.

I. INTRODUCTION

The GaAs(100) surface has attracted much attention due to the large variety of possible surface reconstructions.[1] Extensive studies by reflection high-energy electron diffraction,[2,3] low-energy electron diffraction (LEED),[1] medium-energy ion scattering,[4] scanning tunneling microscopy (STM),[5,6] high-resolution electron energy-loss spectroscopy,[7,8] angular resolved photoemission spectroscopy,[9–11] and reflectance difference spectroscopy (RDS),[12–14] as well as theoretical calculations[15–18] have been performed in order to clarify the atomic and electronic structure of the (100) surface. Unfortunately, a conclusive picture has not yet emerged. On the one hand, the GaAs(100) surface is difficult to prepare reproducibly without the availability of molecular beam epitaxy (MBE) growth equipment, on the other hand the theoretical approach is complicated due to the large surface unit cells of the real structures.

The dimerization of the outermost atomic layer gives rise to various reconstructions which depend strongly on the surface stoichiometry (As or Ga content, respectively). Three main reconstructions, the Ga-rich (4×2), the As-rich (2×4) (β phase), and the As-rich $c(4 \times 4)$, are frequently found and used for surface studies. The outermost atomic layers of the Ga-rich (4×2) [or As-rich (2×4)] reconstructions consist of 0.75 ML of Ga (As) arranged in dimers along [011] ($[0\bar{1}1]$). The As-rich $c(4\times4)$ surface consists of 0.75 ML of As on top of one complete As layer forming dimers in the [011] direction.[5,18] A schematic picture of the structural model of the $c(4\times4)$ surface is diplayed in Fig. 1.[5]

It has been shown recently that RDS is a very sensitive optical tool for the investigation of the GaAs(100) surface reconstructions.[12–14,19,20] RDS monitors the difference between the reflectivity along the principal crystal axes in the surface normalized to the average reflectivity: $\Delta R/R = (R_{[0\bar{1}1]} - R_{[011]})/\bar{R}$.[21] For cubic semiconductors, such as GaAs, the RDS signal is surface specific since, to a good approximation, the bulk reflectivity is isotropic.[22] The dimers of the reconstructed GaAs(100) surfaces cause characteristic features in the optical surface anisotropy.[12,13] In a simplified picture, the surface anisotropy of the dimers is due to larger polarizability along the dimer bonds as compared to that perpendicular. Therefore the sign of the RDS signal reveals the orientation of the bonds. The spectral position of optical transitions related to dimer states is characteristic

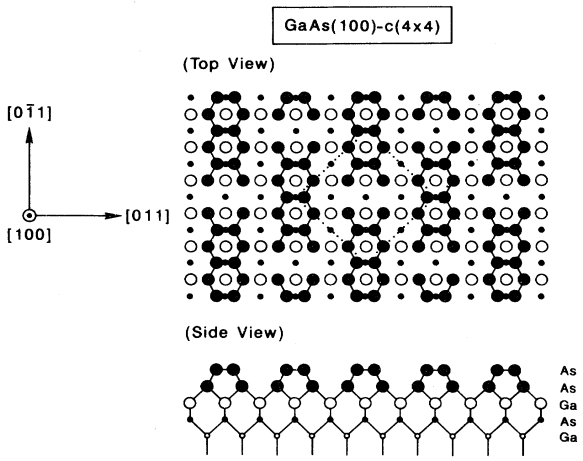

FIG. 1. Schematic view of the atomic arrangement of the GaAs(100)-$c(4 \times 4)$ surface. The outermost layer consists of 0.75 ML As forming dimers along the [011] direction. The dotted lines indicate the $c(4 \times 4)$-surface unit cell (from Ref. 5).

for the involved atomic species (i.e., Ga or As). In order to provide a microscopic understanding of the RDS spectra, the optical anisotropy of the dimerized surfaces was theoretically determined on the basis of surface band-structure calculations.[17,18] However, so far the agreement with experimental results is rather poor, thus preventing a conclusive interpretation of the surface anisotropy.

The study of atomic hydrogen adsorption on GaAs(100)-$c(4 \times 4)$ is another approach to gain some understanding of the origin of the surface optical anisotropy. Atomic hydrogen is known to break the As dimers and to saturate the dangling bonds at the surface.[7,23,24] Therefore the study of the changes induced by hydrogen adsorption in the RDS spectra should allow us to identify the origin of the optical anisotropy.

In this paper we report the results of a study of the hydrogen adsorption on GaAs(100)-$c(4 \times 4)$ by RDS and LEED. The LEED pattern monitors the changes in the structure induced by hydrogen adsorption while the changes in the optical properties are recorded simultaneously by RDS. While these techniques probe completely different properties of the surface, they are complementary in the sense that LEED is sensitive to long-range order of the surface whereas RDS reflects rather the local structure.

II. EXPERIMENT

Undoped and Si-doped n-type ($n = 1 \times 10^{17}$ cm^{-3}) homoepitaxial GaAs layers (1 μm thick) were grown by MBE on GaAs(100) substrates and capped with a 60–100 nm thick As layer deposited by an As_2-cracker cell. After capping, the samples were transferred in air to the UHV analysis chamber where the LEED and RDS experiments were performed. Clean, $c(4 \times 4)$ reconstructed GaAs(100) surfaces were prepared by thermal annealing of the samples to approximately 350 °C.[25] This technique has been tested extensively in recent work and is a well-established method for the reproducible preparation of well-defined (100) surfaces.[6,11,13,25] In fact, recent STM investigations on As-rich (2×4)-reconstructed surfaces prepared by As decapping of the same GaAs(100) samples as studied here show a well-ordered surface structure of comparable quality to *in situ* STM observations on MBE-grown surfaces.[26,27] Hydrogen adsorption was achieved by exposure to atomic hydrogen, created from molecular hydrogen at a hot tungsten filament about 10 cm away from the sample. We express the exposure in Langmuir (1 L=10^{-6} Torr $H_2 \times$ 1 s).

LEED patterns were taken with a PC controlled VIDEO-LEED system equipped with a high sensitive video camera, and a four-grid, reverse-view optic. The reflection anisotropy was recorded in the spectral range of 1.5–5.5 eV using a compact spectrometer unit which consists of a Xe lamp, a single grating monochromator, a photoelastic modulator, Rochon prisms, and a photomultiplier.[20]

III. RESULTS

Figure 2 displays the RDS spectra of undoped (a) and doped n-type GaAs(100) (b) with $c(4 \times 4)$ reconstructed surfaces which were exposed to various amounts of hydrogen. The observed LEED pattern is given for each hydrogen exposure. The RDS spectra of the undoped and doped samples develop in a very similar fashion with hydrogen exposure. However, in the 2.9–3.1 eV range a structure is present which is much more pronounced for the doped sample [Fig. 2(b)]. We find the electric field within the surface depletion region to be responsible for this effect, as will be discussed below. For the undoped sample the electric field effect should be negligible. The optical anisotropy of the $c(4 \times 4)$ reconstructed surface exhibits a characteristic line shape, showing a pronounced minimum around 2.7 eV, and a maximum around 4 eV. Both of these features appear to be unaffected by hydrogen adsorption up to 10 L. In this exposure range the $c(4 \times 4)$ LEED pattern becomes even more distinct due to a reduction of the diffuse background. Increasing the hydrogen exposure to 100 L results in a flattening of the 4 eV maximum of the reflectance anisotropy together with a weakening of the $c(4 \times 4)$ LEED pattern. At higher hydrogen exposures, around 400 L, the reflectance anisotropy is significantly reduced over the whole spectral range. The surface is, possibly fortuitously, nearly isotropic for the exposure of 400 L in the data of Fig. 2(b). The remaining structures occur predominantly around the bulk critical points, while the corresponding LEED pattern shows a (1×1) reconstruction. Hydrogen exposures of 1000 L and 4000 L induce a new surface anisotropy. Two minima develop around 2.4 eV and at 4.1 eV. Also the LEED experiments reveal the appearance of a new surface anisotropy at these exposures. Figure 3 shows a photograph of the LEED pattern and the corresponding schematic diagram. We attribute the LEED pattern to a mixture of two reconstructions

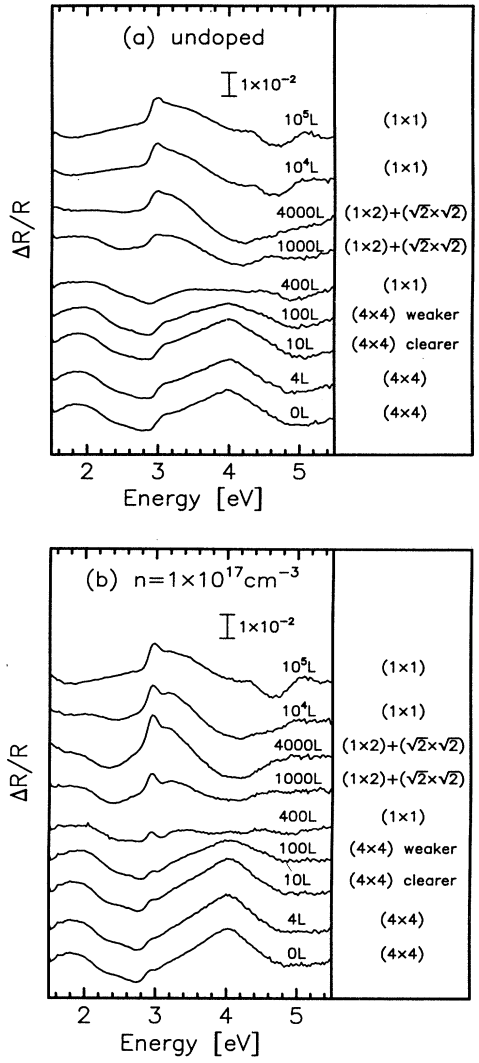

FIG. 2. Reflectance anisotropy $\Delta R/R = 2\mathrm{Re}(\Delta r/r) = (R_{[0\bar{1}1]} - R_{[011]})/\bar{R}$ (r complex reflectivity as determined by RDS) of undoped (a) and $n = 1 \times 10^{17}$ cm^{-3}-doped n-type GaAs(100) (b) with $c(4 \times 4)$ reconstructed surfaces exposed to various amounts of hydrogen. The observed LEED pattern is given for each hydrogen exposure.

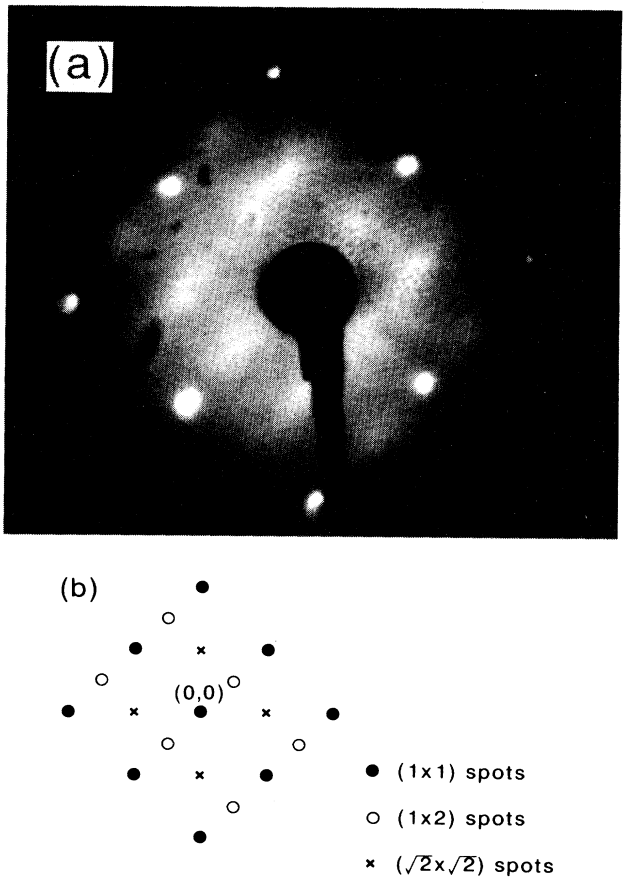

FIG. 3. (a) LEED pattern observed between 1000 L and 4000 L hydrogen exposure. We propose that the LEED pattern is composed of two superstructures which originate from (1×2) and from $(\sqrt{2} \times \sqrt{2})$ surface domains. The schematic figure (b) demonstrates how the original LEED pattern is generated by the superposition of the two reconstructions.

of (1×2) and $(\sqrt{2} \times \sqrt{2})$ domains, as will be discussed below in more detail. These reconstructions disappear at higher hydrogen exposures (i.e., 10^4 L and 10^5 L) where a (1×1) LEED pattern reappears. In the RDS spectra the surface anisotropies at 2.4 eV, and 4.1 eV are removed and instead, new features around the bulk critical points are observed (E_1 at 2.91 eV, $E_1 + \Delta_1$ at 3.14 eV, E_0' at 4.44 eV and E_2 at 4.96 eV).[30]

IV. DISCUSSION

Both the reflectance anisotropy and the LEED pattern reveal drastic changes of the GaAs(100)-$c(4 \times 4)$ surface upon exposure to hydrogen. Before discussing the RDS results, we give a brief review of the present understanding of the $c(4 \times 4)$ surface (Fig. 1) and the corresponding RDS spectrum (see Fig. 2, bottom spectra). The atomic structure of the GaAs-$c(4 \times 4)$ surface, as determined by STM,[5] is illustrated in Fig. 1. The first two atomic layers both consist of As atoms. In the outermost layer As dimers are formed along the [011]-direction, whereas bonds between the first and second As layer are mainly oriented along $[0\bar{1}1]$. RDS studies performed *in situ* in a MBE system revealed two different line shapes of RDS spectra of a $c(4 \times 4)$ reconstruction depending on the substrate temperature.[12] The difference in the RDS spectrum at lower temperature was tentatively assigned to the influence of As adatoms additionally adsorbed on random sites on top of the $c(4 \times 4)$ surface and termed as $d(4 \times 4)$ structure (d equals disordered).[12] The bottom spectra in Fig. 2 (clean surface) show the typical line shape of this so-called $d(4 \times 4)$ spectrum. The RDS minimum around 2.7 eV has been attributed to electronic transitions of the As-dimer bonds in the outermost layer, whereas the maximum around 4 eV has not yet been assigned.[12] Band-structure calculations based on a sim-

plified (1×2) surface reconstruction suggest that both structures are due to electronic transitions of the As dimers.[31] However, experimentally, when comparing the $c(4 \times 4)$ (dimers along [011]) with the (2×4) reconstruction (dimers along $[0\bar{1}1]$) the expected inversion of the sign of the dimer features does not occur at 4 eV, in contrast to the 2.7 eV feature.

In accordance with a recent high-resolution electron-energy-loss spectroscopy (HREELS) study (Ref. 7), the evolution of the RDS spectrum upon hydrogen exposure shown in Fig. 2 can be separated into four different regimes which are related to a layer-by-layer etching of the $c(4 \times 4)$ surface, most probably by desorption of AsH_3.[42]

At low exposures, up to 10 L, the $c(4\times4)$ LEED pattern becomes clearer. The sharpening of the LEED pattern indicates the removal of disordered As adatoms which stick on top of the ordered $c(4 \times 4)$ structure. Since the $c(4 \times 4)$ surface is prepared by a thermal desorption of a thick As_2-cap layer, the origin of the As atoms in excess of the ordered structure can be safely attributed to an incomplete desorption. Remarkably, the line shape of the RDS spectra is not affected by the improvement of surface ordering due to the removal of the excess As. Therefore, in contrast to previous suggestions, the different line shapes of the so-called $d(4\times4)$-RDS and $c(4\times4)$-RDS spectra are most likely attributed to other effects than surface disorder. Also, recent studies by grazing incidence x-ray diffraction (GIXD) (Refs. 28 and 29) performed in a metal-organic vapor phase epitaxy (MOVPE) environment did not reveal the existence of a disordered $c(4 \times 4)$ structure. The GIXD experiments indicate that the $c(4 \times 4)$ surface is not necessarily composed of three As dimers per unit cell, but can also contain only two dimers. Therefore, we suspect that either the number of As dimers or simply the elevated substrate temperature of the *in situ* MBE- and MOVPE-RDS experiments in contrast to room temperature in the present experiments are relevant for the different spectral shape of the so-called $d(4 \times 4)$ and $c(4 \times 4)$. In agreement with this conjecture, a recent UHV-RDS study reports a surface optical anisotropy of the $c(4 \times 4)$ which is almost identical to that found here.[13] Therefore, we believe that the bottom spectra in Fig. 2 can be attributed to an ordered $c(4 \times 4)$ surface structure at room temperature. A combined study by RDS and STM would help to clarify the microscopic origin of the difference in the RDS spectra.

In a second regime of exposures, from 10 L up to 400 L, a weakening of the fractional order spots of the $c(4 \times 4)$ LEED pattern occurs, finally leading to a (1×1) pattern with low background. This indicates the removal of the As dimers in the outermost layer. A new dimerization of the remaining As layer, which could be identified by RDS features similar to those found for the As-rich (2×4) surface, is most likely inhibited since the dangling bonds are saturated with hydrogen. The weakening of the fractional order spots of the $c(4 \times 4)$ LEED pattern is accompanied by a reduction of the maximum at 4 eV in the RDS spectrum. At 400 L, where a clear (1×1) pattern is established, the minimum at 2.7 eV is also reduced. Thus, in this second exposure regime, the As dimers are removed and the surface consists most likely of a hydrogen terminated (1×1) As monolayer. The hydrogen-induced modification of the RDS spectra clearly demonstrates that both the 2.7 eV and 4 eV features result from surface electronic states which originate from the outermost As layer. The retarded supression of the minimum at 2.7 eV, as compared to the 4 eV peak, can be understood if the 4 eV maximum is tentatively attributed to the As-As backbonds of the first to second As layer. In this case, hydrogen would firstly break the backbonds, reducing the spectral response at 4 eV, while the As dimers in the first layer would be removed after several of these backbonds are broken, thus reducing the spectral response of the 2.7 eV minimum at higher exposures. This suggestion would agree with the simple argument of bond direction: the As-As backbonds are oriented along the $[0\bar{1}1]$ direction and thus would give a positive contribution, i.e., maximum, while the As-As dimers oriented along [011] would give a negative contribution, i.e., a minimum in the reflection difference as observed here (Fig. 1). Alternatively, the initial reduction of the surface anisotropy at 4 eV for lower H exposures could also be understood if this feature were characteristic for a three-dimer $c(4 \times 4)$ unit cell. In this approach, the hydrogen at low exposures would simply reduce the number of unit cells occupied by three As dimers leading to a larger number of two-dimer unit cells before the dimers are completely removed. Summarizing the intermediate exposure regime, the lifting of the surface anisotropy clearly demonstrates the removal of the outermost As dimers and the H passivation of the residual As dangling bonds preventing a new dimerization at the surface. The detailed interaction mechanism of H with the As dimers, however, cannot be clarified by RDS experiments alone and needs further investigations, e.g., by STM.

When increasing the hydrogen exposure to the 1000–4000 L range, a new type of surface anisotropy appears. The RDS spectrum changes significantly, showing now an additional minimum around 2.4 eV. From RDS studies on Ga rich (4×2) surfaces[13,14] and calculated RDS spectra[17,18] this minimum is well known to represent the signature of Ga dimers formed along the [011] direction on the surface. We attribute the LEED pattern to a superposition of (1×2) and $(\sqrt{2} \times \sqrt{2})$ domains (Fig. 3), which is consistent with the appearance of Ga dimers. Figure 4 shows two possible arrangements of Ga dimers which give rise to a (1×2) and a $(\sqrt{2} \times \sqrt{2})$ reconstruction. Consequently, in the third exposure range (1000–4000 L) the As layer is removed by hydrogen etching and the surface is composed of Ga dimers, at least to a large extent. In excellent agreement with these results, HREELS studies of hydrogen adsorption on GaAs(100)-$c(4\times4)$ surfaces showed the complete removal of the outermost As layers and the indication of a (1×2) LEED pattern.[7]

The formation of a Ga-dimer-terminated GaAs(100) surface by hydrogen etching suggests that the As–H bonding is more favorable than the Ga–H bonding. Nevertheless, for even higher exposures, up to 10^4 L or 10^5 L, the Ga dimers decompose by hydrogenation. This is in-

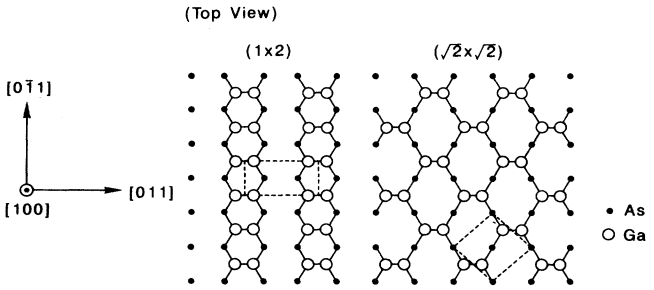

FIG. 4. Arrangement of Ga dimers on the GaAs(100) surface in (1×2) and $(\sqrt{2} \times \sqrt{2})$ surface domains. The surface unit cells are indicated by dotted lines.

dicated by the development of a (1×1)-LEED pattern, as well as by the removal of the Ga-dimer related features in the RDS spectra. The surface anisotropy shows features predominantly in the region of the bulk critical points, similar to those reported for sulphur-exposed GaAs(100) surfaces.[32] This suggests that the anisotropy originates from surface-induced modifications of the wave functions and matrix elements of the bulk states in the surface region.[33,34] At these large exposures the layer-by-layer etching is replaced by the onset of inhomogenous surface etching inducing a disordered, microrough surface.[34,35] In spite of the fact that for large as well as for 400 L of H exposures the microscopic surface anisotropy due to surface dimers is removed, the surface roughness causes the RDS spectra at large H exposures to differ significantly from those around 400 L.

For the doped sample a distinct structure is present around 3.0 eV in the RDS spectra, i.e., in the vicinity of the E_1 and $E_1 + \Delta_1$ bulk critical points. It has been shown in previous RDS studies[13,36–38] that the electric field in the surface band bending region (present due to surface Fermi level pinning) is responsible for this feature. In fact, the surface Fermi level is known to lie around midgap on the clean and hydrogenated GaAs(100) surface.[7,13,39] As can be shown by symmetry arguments,[40] only the linear electro-optic effect results in an optical anisotropy, whereas the quadratic one is isotropic on the (100) surface. The electric field induced change in dielectric function can be written as[41]

$$\begin{aligned} \Delta\epsilon_{[011]} &= \tfrac{1}{2}\chi_{123}\mathcal{E}, \\ \Delta\epsilon_{[0\bar{1}1]} &= -\tfrac{1}{2}\chi_{123}\mathcal{E}, \end{aligned} \tag{1}$$

where χ_{123} represents the only nonzero element of the third-rank susceptibility tensor and $\mathcal{E}$ the electric field strength. Calulations of χ_{123} can be found in Ref. 37. For the undoped sample (background doping: $n \approx 1 \times 10^{15}$ cm^{-3}) the electric field effect is negligible.[38]

V. CONCLUSION

We have investigated the hydrogen-induced change of the GaAs(100)-$c(4 \times 4)$ surface and found an initial improvement in ordering and then its stepwise degradation. For low exposures, hydrogen is found to remove As by etching off the surface. This allows us to get a clearer understanding of the origin of the surface anisotropy. At first, the outermost 0.75 ML As-dimer layer is removed and an isotropic, hydrogen-terminated surface is formed. We find that both the 2.7 eV minimum and the 4 eV maximum in the reflectance anisotropy of the $c(4 \times 4)$ surface originate from surface states related to the outermost As layer. At intermediate hydrogen exposures the As surface layer is completely removed and Ga dimers arrange in (1×2) and $(\sqrt{2} \times \sqrt{2})$ domains terminating the surface. For high exposures, the Ga dimers are finally broken and a surface roughening occurs which is reflected in the optical anisotropy of the surfaces.

ACKNOWLEDGMENTS

We are indebted to U. Resch-Esser for helpful discussions about the LEED results and the preparation of the GaAs(100) surfaces by As decapping. We would like to thank J. Zegenhagen and S. Donovan for a critical reading of the manuscript.

[1] P. Drathen, W. Ranke, and K. Jacobi, Surf. Sci. **77**, L162 (1978).
[2] A. Y. Cho, J. Appl. Phys. **47**, 2841 (1976).
[3] J. M. Van Hove, P. I. Cohen, and C. S. Lent, J. Vac. Sci. Technol. A **1**, 546 (1983).
[4] J. Falta, R. M. Tromp, M. Copel, G. D. Pettit, and P. D. Kirchner, Phys. Rev. Lett. **69**, 3068 (1992).
[5] D. K. Biegelsen, R. D. Bringans, J. E. Northtrup, and L.-E. Swartz, Phys. Rev. B **41**, 5701 (1990).
[6] S. L. Skala, J. S. Hubacek, J. R. Tucker, J. W. Lyding, S. T. Chou, and K. Y. Cheng, Phys. Rev. B **48**, 9138 (1993).
[7] J. A. Schaefer, F. Stietz, J. Woll, H. S. Wu, H. Yu, and G. J. Lapeyre, J. Vac. Sci. Technol. B **11**, 1497 (1993).
[8] L. H. Dubois and G. P. Schwartz, Phys. Rev. B **40**, 8336 (1989).
[9] P. K. Larsen, J. F. van der Veen, A. Mazur, J. Pollmann, J. H. Neave, and B. A. Joyce, Phys. Rev. B **26**, 3222 (1982).
[10] P. K. Larsen, J. H. Neave, J. F. van der Veen, P. J. Dobson, and B. A. Joyce, Phys. Rev. B **27**, 4966 (1983).
[11] G. Le Lay, D. Mao, A. Kahn, Y. Hwu, and G. Margaritondo, Phys. Rev. B **43**, 14 301 (1991).
[12] I. Kamiya, D. E. Aspnes, L. T. Florez, and J. P. Harbison, Phys. Rev. B **46**, 15 894 (1992).
[13] U. Resch, S. M. Scholz, U. Rossow, A. B. Müller, and W. Richter, Appl. Surf. Sci. **63**, 106 (1993).
[14] I. Kamiya, D. E. Aspnes, H. Tanaka, L. T. Florez, J. P. Harbison, and R. Bhat, Phys. Rev. Lett. **68**, 627 (1992).
[15] D. J. Chadi, J. Vac. Sci. Technol. A **5**, 884 (1987).
[16] P. K. Larsen and D. J. Chadi, Phys. Rev. B **37**, 8282 (1988).
[17] Y.-C. Chang and D. E. Aspnes, Phys. Rev. B **41**, 12 002 (1990).
[18] Y.-C. Chang, S.-F. Ren, and D. E. Aspnes, J. Vac. Sci. Technol. A **10**, 1856 (1992).
[19] D. E. Aspnes, J. Sci. Vac. Technol. B **3**, 1502 (1985).
[20] S. M. Scholz, A. B. Müller, W. Richter, D. R. T. Zahn, D.

I. Westwood, D. A. Woolf, and R. H. Williams, J. Vac. Sci. Technol. **B 10**, 1710 (1992).
[21] D. E. Aspnes, J. P. Harbison, A. A. Studna, and L. T. Flores, J. Vac. Sci. Technol. A **6**, 1327 (1988).
[22] P. Y. Yu and M. Cardona, in *Computational Solid State Physics*, edited by F. Herman, N. W. Dalton, and T. R. Koehler (Plenum Press, New York, 1972).
[23] R. Z. Bachrach and R. D. Bringans, J. Phys. **C5**, 145 (1982).
[24] H. Qi, P. E. Gee, and R. F. Hicks, Phys. Rev. Lett. **72**, 250 (1994).
[25] U. Resch, N. Esser, Y. S. Raptis, W. Richter, J. Wasserfall, A. Förster, and D. I. Westwood, Surf. Sci. **269/270**, 797 (1992).
[26] U. Resch-Esser, C. Springer, W. Richter, N. Esser, J. Zegenhagen, M. Cardona, and B. O. Fimland, J. Vac. Sci. Technol. B (to be published).
[27] T. Hashizume, Q. K. Xue, J. Zhou, A. Ishimiya, and T. Sakurai, Phys. Rev. Lett. **73**, 2208 (1994).
[28] A. P. Payne, P. H. Fuoss, D. W. Kisker, G. B. Stephenson, and S. Brennan, Phys. Rev. B **49**, 14 427 (1994).
[29] F. J. Lamelas, P. H. Fuoss, D. W. Kisker, G. B. Stephenson, P. Imperatori, and S. Brennan, Phys. Rev. B **49**, 1957 (1994).
[30] P. Lautenschlager, M. Garriga, S. Logothetidis, and M. Cardona, Phys. Rev. B **36**, 4813 (1987).
[31] Y.-C. Chang and D. E. Aspnes, J. Vac. Sci. Technol. B **8**, 896 (1990).
[32] G. Hughes, C. Springer, U. Resch-Esser, N. Esser, and W. Richter, J. Appl. Phys. (to be published).
[33] F. Manghi, E. Molinari, R. Del Sole, and A. Selloni, Phys. Rev. B **39**, 13 005 (1989).
[34] M. Kuball, M. K. Kelly, P. V. Santos, and M. Cardona, Phys. Rev. B **50**, 8609 (1994).
[35] J. A. Schaefer, T. Allinger, C. Stuhlmann, U. Beckers, and H. Ibach, Surf. Sci. **251/252**, 1000 (1991).
[36] V. L. Berkovits, V. N. Bessolov, T. N. L'vova, E. B. Novikov, V. I. Safarov, R. V. Khasieva, and B. V. Tsarenkov, J. Appl. Phys. **70**, 3704 (1991).
[37] H. Tanaka, E. Colas, I. Kamiya, D. E. Aspnes, and R. Bhat, Appl. Phys. Lett. **59**, 3443 (1991).
[38] S. E. Acosta-Ortiz and A. Lastras-Martinez, Phys. Rev. B **40**, 1426 (1989).
[39] W. Chen, M. Dumas, D. Mao, and A. Kahn, J. Vac. Sci. Technol. B **10**, 1886 (1992).
[40] J. F. Nye, *Physical Properties of Crystals* (Oxford University Press, Oxford, 1976), pp. 110ff.
[41] D. S. Kyser and V. Rehn, Solid State Commun. **8**, 1437 (1970).
[42] J. R. Creighton, J. Vac. Sci. Technol. A **8**, 3984 (1990).

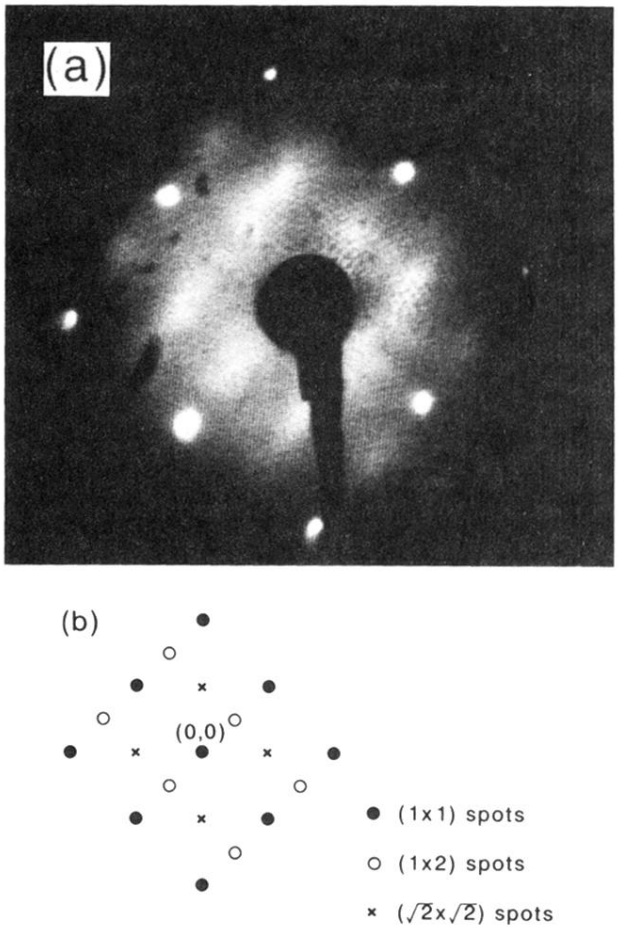

FIG. 3. (a) LEED pattern observed between 1000 L and 4000 L hydrogen exposure. We propose that the LEED pattern is composed of two superstructures which originate from (1×2) and from $(\sqrt{2} \times \sqrt{2})$ surface domains. The schematic figure (b) demonstrates how the original LEED pattern is generated by the superposition of the two reconstructions.